Energy 197 (2020) 117232

Contents lists available at ScienceDirect

Energy

journal homepage: www.elsevier.com/locate/energy

Use of exergy efficiency for the optimization of LNG processes with NGL extraction

Donghoi Kim, Truls Gundersen*

Department of Energy and Process Engineering, Norwegian University of Science and Technology (NTNU), Kolbjørn Hejes Vei 1B, NO-7491, Trondheim, Norway

ARTICLE INFO

Article history:
Received 12 June 2019
Received in revised form
17 January 2020
Accepted 22 February 2020
Available online 25 February 2020

Keywords:
Energy efficiency
Exergy efficiency
Natural gas liquefaction
Dual mixed refrigerant process
Heavy hydrocarbon removal
Exergy optimization

ABSTRACT

In this paper, processes for liquefied natural gas (LNG) production with upstream or integrated natural gas liquids (NGL) removal have been optimized and compared. Since the NGL and LNG production systems use both work and heat to deliver products with different energy quality, it is challenging to measure accurately the thermodynamic efficiency by using conventional energy performance indicators. Thus, two different objective functions, specific energy consumption and exergy efficiency, have been applied in the optimization of these complex systems in order to evaluate the effectiveness of the two performance indicators. The results indicate that use of the exergy-based objective function results in a richer NGL and a larger amount of LNG production with a marginal increase in energy consumption, showing a higher thermodynamic efficiency than the result with the energy-based objective function. Besides, integrated NGL extraction shows a lower thermodynamic performance than upstream removal, indicating that further advanced schemes are required for effective integration of the NGL extraction part in the LNG process.

1. Introduction

The main objective of this paper is to introduce and evaluate exergy as a key performance indicator that can be used to optimize complex industrial processes. Exergy is defined as the maximum amount of work that can be obtained when a system is brought to equilibrium with its surroundings (i.e. temperature, pressure and chemical composition). Thus, exergy measures both the amount (1st Law of Thermodynamics) and quality (2nd Law of Thermodynamics) of energy, and it will be compared with specific energy consumption that is often used in the process industries. Of course, the ultimate performance parameter for industrial processes is Total Annualized Cost (TAC), however, simpler criteria are often used in conceptual design.

One significant advantage with exergy compared to energy is the ability to consider both energy and material streams. It can also distinguish different energy forms such as work and heat, the latter having a quality that depends strongly on its temperature level. In subambient processes, thermodynamic inefficiencies translate into exergy losses that directly affects compression work in the refrigeration cycles. Thus, processes for liquefaction of natural gas are prime candidates for use of exergy efficiency as performance indicator. These processes operate below ambient, they have two main products (LNG – Liquefied Natural Gas and NGL – Natural Gas Liquids), and they use both work for compression and heat for fractionation. The LNG and NGL products vary in volume and composition depending on the plant configuration and operating parameters. Most of these processes also have complex flowsheet structures.

2. Natural gas liquefaction with heavier hydrocarbon extraction

For global energy security, natural gas is one of the important energy sources with high mobility in the form of liquid [1]. During the liquefaction of natural gas, heavier hydrocarbons (HHC) like natural gas liquids (NGL) are often extracted from the feed gas. The extraction is performed to prevent the freeze-out of HHCs in the liquefier and control the heating value of the liquefied natural gas (LNG) to meet the export specifications. The recovered HHCs are treated and sold as an additional product (NGL), improving project profitability due to the high economic value of these components. In addition, the hydrocarbons from the extraction schemes are

* Corresponding author.
E-mail address: truls.gundersen@ntnu.no (T. Gundersen).

https://doi.org/10.1016/j.energy.2020.117232

further fractionated and partly used as make-up for the refrigerants in the LNG process.

NGL recovery from natural gas can be conducted upstream or as an integral part of the liquefaction system. The former scheme is achieved by a Joule-Thomson valve, a gas expander, and a scrub column. The latter requires an integration of the NGL extraction process with the LNG process, which may increase the complexity of design and operation. Traditionally, upstream NGL extraction systems were proposed for pipeline gas production as one of the treatment steps. Some of the typical systems are the industry standard single stage (ISS) process [2], the gas sub-cooled process (GSP) [3], and the recycle split vapor (RSV) process [4]. Since the upstream NGL systems were not originally designed for LNG processes, various configurations for the integration of NGL recovery schemes in LNG processes have also been suggested. Ghorbani et al. apply absorption refrigeration to reduce heat demand in the distillation column for NGL extraction [5]. Ghorbani et al. also propose an integrated scheme for LNG production, NGL extraction, and nitrogen removal process [6]. Uwitonze et al. suggest different ways of heat integration between LNG and NGL processes [7]. There is also a thermally-coupled NGL extraction with a LNG process by splitting the feed stream [8].

Nevertheless, there have been very few studies providing a comparative analysis of the two types of NGL extraction systems (upstream and integrated NGL processes). Most studies have focused on a comparison between the various upstream NGL recovery configurations. Shin et al. compare the GSP, RSV, and their modified concept (cold residue reflux process) based on exergy loss [9]. Park et al. perform cost analysis for 10 different configurations of upstream NGL extraction including the ISS, GSP, and RSV [10]. Kim et al. evaluate simplified NGL extraction schemes using Joule-Thomson valves, a gas expander, and a scrub column [11].

This motivated an optimization study based on cost analysis in order to compare the upstream and the integrated schemes [12]. However, their work does not indicate the maximum achievable thermodynamic performance of the two different schemes, which could have been the basis for process improvement. Therefore, this paper provides a comparative thermodynamic analysis for the two types of NGL extraction systems (upstream and integrated) by performing optimization studies.

The NGL recovery processes tend to be analyzed [11] and optimized [7,8,13–16] using an energy performance indicator (power consumption) to improve the systems. However, the energy efficiency for such cryogenic systems does not accurately reflect the thermodynamic performance of the processes since the indicator is not able to include the quality of the heat supplied (temperature) and the products (temperature, pressure, and composition) [17,18]. The direct comparison of heat at different temperature levels with electric power is another undesirable property of the energy performance indicator for NGL extraction systems where both heat and power are consumed. Thus, exergy efficiency is selected as objective function for the optimization of the NGL and LNG production systems [17]. For the natural gas liquefaction part, a dual mixed refrigerant (DMR) LNG process is selected and optimized

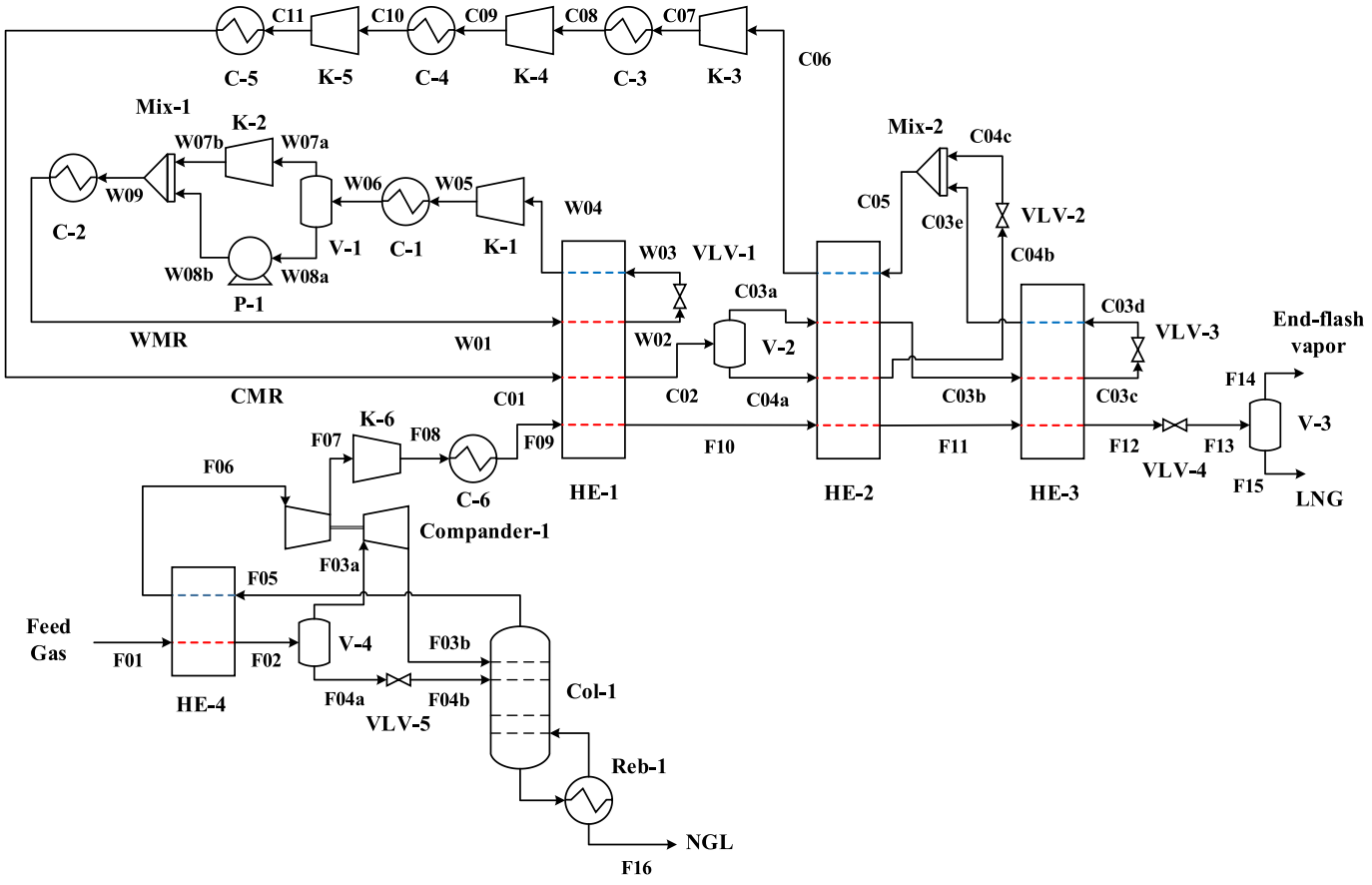

Fig. 1. Process flow diagram of the DMR process with upstream NGL extraction (ISS-LNG system [2,3]).

together with the NGL recovery systems.

3. Process design alternatives

3.1. DMR process with upstream NGL extraction

The upstream HHC extraction is typically performed by gas expander based systems. Through turbo-machinery equipment, the temperature of the feed gas is reduced due to the expansion, supplying the cold duty of the NGL extraction system. Thus, there have been various extraction schemes using gas expanders [2–4,19]. In this work, we choose a simple upstream NGL extraction system referred to as the industry standard single stage (ISS) process in order to focus on the fundamental differences between upstream and integrated configurations [2,3]. A DMR process [20] is selected and integrated with the ISS scheme in order to represent the liquefaction system in this work. This liquefaction process contains two refrigeration cycles having mixed hydrocarbon refrigerants.

Fig. 1 shows the entire system for upstream NGL extraction and LNG production, which is referred to as the ISS-LNG system. The feed gas is sent to heat exchanger HE-4 and cooled to be partially condensed. The two-phase mixture stream is then separated to vapor (F03a) and liquid (F04a) streams in phase separator V-4. The liquid stream is throttled by Joule-Thomson (JT) valve VLV-5 and sent to the top stage of distillation column Col-1 as one of the feed streams. Stream F03a is also expanded through the expander part of a compander (Compander-1) and delivered to the distillation column. A compander is a kind of turbo-machinery where a compressor and expander are installed on the same shaft.

The bottom product from the column is partially vaporized in reboiler Reb-1 to remove lighter hydrocarbons in the NGL product (F15). The heat duty of the re-boiler is assumed to be supplied by steam. The top vapor product from the column is returned to heat exchanger HE-4 to provide its cold duty. Due to the depressurization of the feed gas via the expander and JT valve, the lean vapor product from the column (F06) is recompressed through the compressor part of Compander-1. The compression work is supplied by the power generated during the expansion of stream F03a. Compressor K-6 further boosts the pressure of stream (F07) and sends it to the liquefaction process. The high-pressure lean gas stream (F08) is desuperheated by condenser C-6 and sent to heat exchanger HE-1 to be pre-cooled, and the cooling duty is produced by a refrigeration cycle operated by a warm mixed refrigerant (WMR).

The pre-cooled natural gas is then liquefied through heat exchanger HE-2 and sub-cooled by HE-3. The cold duties of HE-2 and HE-3 are supplied by a refrigeration cycle with a cold mixed refrigerant (CMR). The sub-cooled LNG is then depressurized to near ambient pressure for storage and transportation purposes. The throttled LNG stream F12 is separated in the flash drum (V-3) to a nitrogen rich vapor stream (End-flash vapor) and the LNG product.

3.2. DMR process integrated with NGL extraction

Unlike the ISS-LNG system, the extraction of HHCs can be performed in the middle of the liquefaction system as seen in Fig. 2 [20]. This configuration is referred to as the NGL-LNG system. The feed gas is pre-cooled by heat exchanger HE-1 in the DMR process and throttled by a JT valve (VLV-5). In contrast to the ISS process, the depressurized stream (F03) is sent directly to the top of distillation column Col-1 as a feed stream without any heat integration.

The liquid product extracted from the bottom of the column is then heated in reboiler Reb-1 to vaporize lighter hydrocarbons, and the remaining stream is the NGL product (stream F11). The top vapor stream of Col-1 is compressed in the boost compressor (K-6) to compensate for the reduced pressure level of the feed gas. The pressurized gas stream is then liquefied and sub-cooled in heat exchangers HE-2 and HE-3 before being throttled to ambient pressure to produce end-flash vapor and LNG. In this configuration, the integration of NGL recovery and LNG production allows a

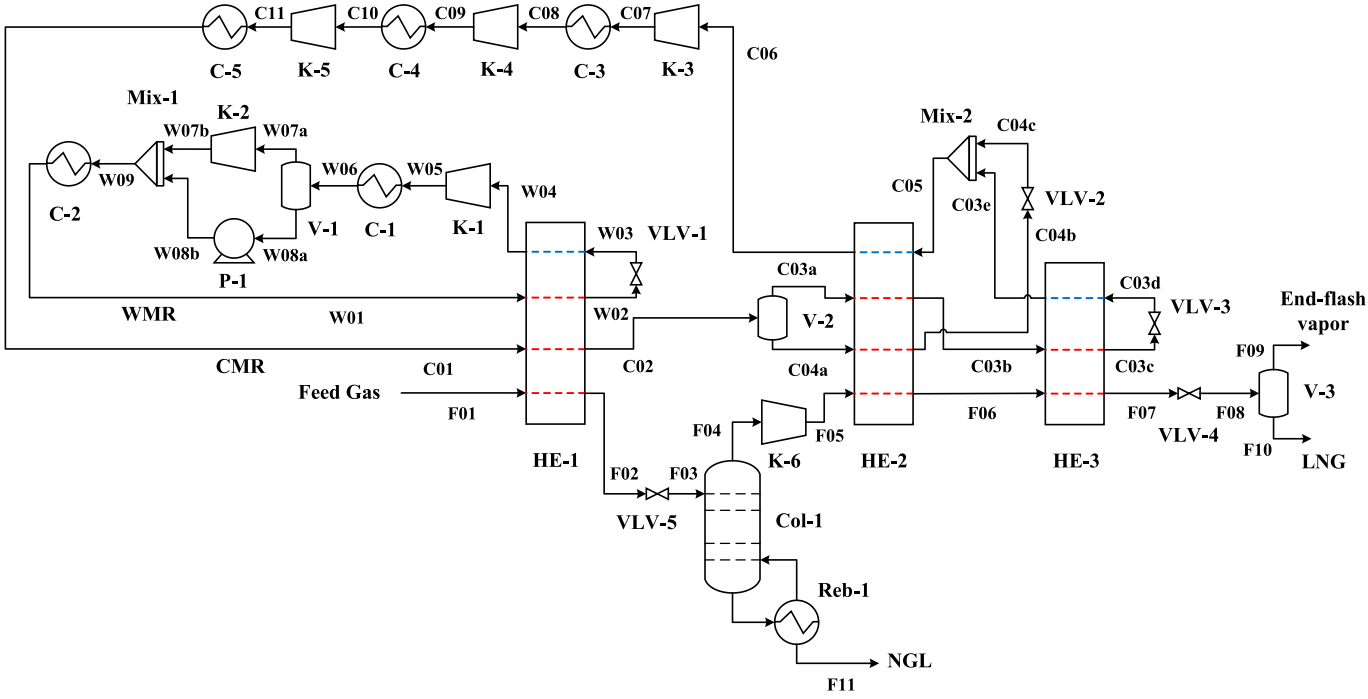

Fig. 2. Process flow diagram of the DMR process integrated with NGL extraction (NGL-LNG system [20]).

reduction in the number of units for HHC extraction compared to the ISS system. However, the performance of the NGL extraction part in this integrated scheme will directly affect the liquefaction process, giving extra difficulties in the optimization and operation of the total system.

3.3. DMR process integrated with refluxed NGL extraction

In order to improve the process efficiency, a refluxed distillation system with a condenser was implemented in the DMR process to be compared with the ISS system. Then, the NGL extraction part of the integrated scheme has the same level of complexity as the ISS-LNG process with the same number of units. This configuration is referred to as the refluxed NGL-LNG system [21]. Similar to the ISS process, the feed gas is cooled by heat exchanger HE-4 as seen in Fig. 3. A portion of the WMR is expanded by JT valve VLV-7 and supplied to HE-4 to cover the cooling demand in the exchanger and then returned to the WMR refrigeration cycle for the DMR process. The cold feed gas is then depressurized through VLV-5 and fed to the top stage of distillation column Col-1. The bottom product of Col-1 is reboiled in heat exchanger Reb-1 to reduce methane slip to the NGL product. The top vapor stream from the column is compressed and sent to heat exchanger HE-1 in the DMR process. The partially condensed feed gas from HE-1 is separated to vapor (F07) and liquid (F13) streams. The liquid stream F13 is returned to the top of the distillation column after being throttled by JT valve VLV-6. This reflux stream (F14) is used to achieve deeper extraction of HHCs from the feed gas. The vapor stream F07 is then further cooled in heat exchangers HE-2 and HE-3 and depressurized in valve VLV-4 to deliver the end-flash vapor stream and the LNG product.

Table 1
Simulation conditions of the integrated schemes.

Design parameters	Unit	Value
Condenser/intercooler outlet	°C	22
Compressor	Polytropic %	78
Pump	Adiabatic %	75
Compressor in a compander	Polytropic %	73
Expander in a compander	Polytropic %	83
Distillation column	Theoretical stages	20

4. Design basis

4.1. Simulation conditions

Natural gas from reservoirs is treated in gas processing plants and delivered to an LNG plant through pipelines. The pipeline gas is sent to gas cleaning stages in the LNG plant where sour gases and water are removed. The pre-treated gas is then fed to the NGL and LNG production systems. Although the gas cleaning steps are essential for the total LNG system, the focus for the simulation and optimization studies in this work is on the NGL and LNG process schemes. Other utility processes of the LNG plant such as end-flash gas handling, power generation, heat production, and cooling water systems were not included in the simulation model. The NGL and LNG production systems were simulated by Aspen HYSYS V9 with the Peng-Robinson equation of state (EOS) [22]. The theoretical number of stages for the NGL extraction column is assumed to be 20 [14]. Pressure drops and heat losses of equipment are neglected in the simulation models. Other simulation conditions for the process units are given in Table 1.

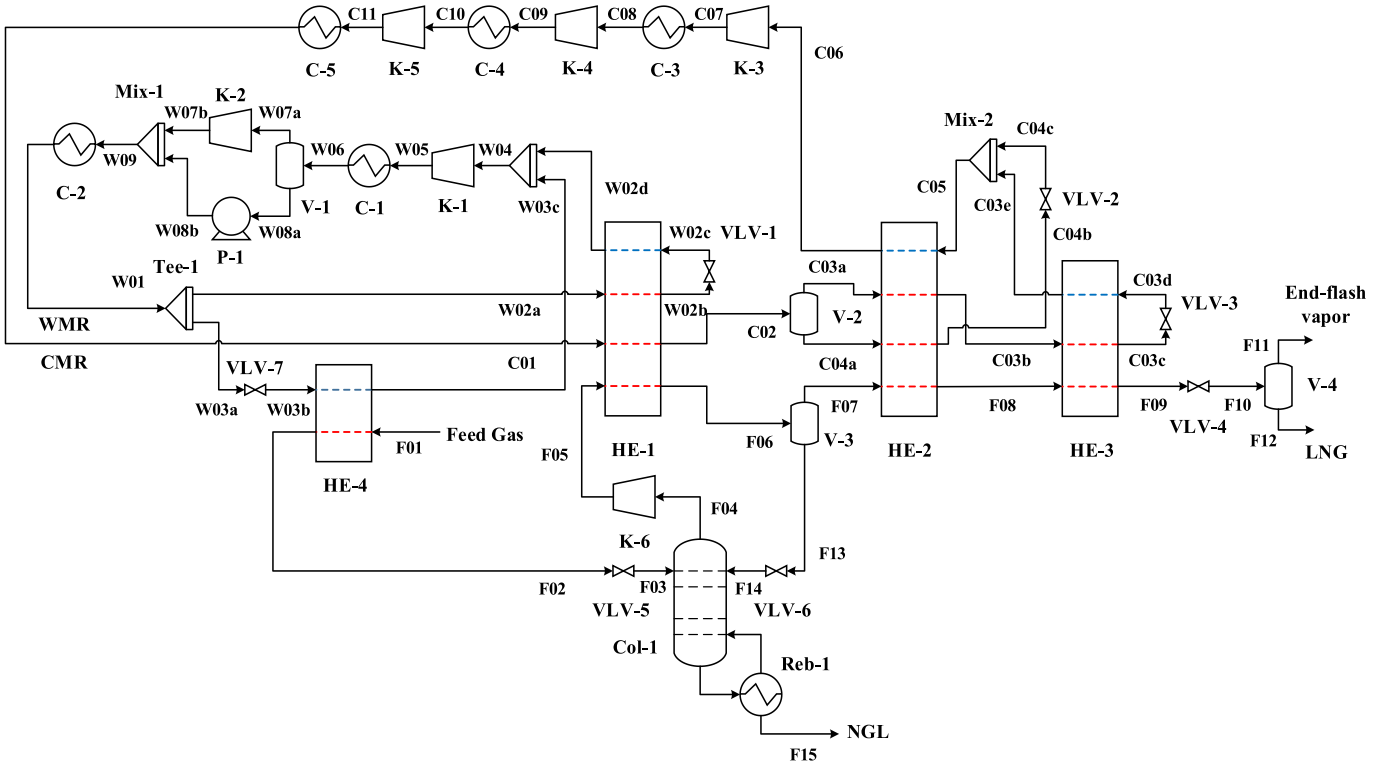

Fig. 3. Process flow diagram of the DMR process integrated with refluxed NGL extraction (refluxed NGL-LNG system [21]).

4.2. Feed gas and products

The removal of benzene, toluene, and xylene (BTX) is essential for NGL extraction systems, since these components easily freeze-out even with marginal fractions during the liquefaction process [23]. Thus, the vapor product from NGL recovery systems have to contain a low level of BTX so that the stream can be liquefied in LNG production systems. However, aromatic hydrocarbon components tend to be excluded in many studies about NGL systems [8–10,12–16,24–27]. Thus, previous research does not guarantee that the gas product from their NGL systems contains a sufficiently small amount of BTX when aromatic components are included in the feed gas. Therefore, in this work, hydrocarbons from methane (C_1) to decane (C_{10}) and the aromatic components (BTX) are included in the feed gas.

As mentioned in Section 4.1, pre-treated gas is sent to the NGL and LNG production systems. Due to the gas cleaning processes, sour components and water are not contained in the feed gas. Other feed gas conditions are seen in Table 2.

To prevent the solidification of HHCs in the LNG process, the amount of BTX in the vapor product from NGL extraction systems is limited to 10 ppm. The fraction of C_{5+} is also set to be smaller than 0.1 mol % in the vapor product in order to maximize the production of NGL, which is more valuable than natural gas and thus LNG due to its higher heating value and the fact that heavier hydrocarbons are used as feedstock for petrochemical products. The pressure level of LNG and end-flash vapor is set to be 1.5 bar for storage and transport purposes. The nitrogen content in the final LNG product is also controlled to be less than 1 mol % to meet sales gas specifications.

5. Performance indicators and optimization

The NGL and LNG production systems are operated by using electric power for compressors and hot steam for the reboiler of the distillation column. During evaluation of these systems, however, the heat delivered by steam is typically disregarded in the calculation of energy performance indicators [7,8,16]. To be more accurate, we use specific energy consumption including heat as an energy performance indicator to evaluate the NGL extraction and LNG process [28].

Table 2
Feed gas conditions.

Property	Unit	Value
Temperature	°C	22.00
Pressure	bar	60.00
Flow rate	kmol/hr	35000.00
Nitrogen	mol %	1.00
Methane	mol %	91.00
Ethane	mol %	4.90
Propane	mol %	1.70
i-Butane	mol %	0.35
n-Butane	mol %	0.40
i-Pentane	mol %	0.15
n-Pentane	mol %	0.15
n-Hexane	mol %	0.13
n-Heptane	mol %	0.10
n-Octane	mol %	0.04
n-Nonane	mol %	0.01
n-Decane	mol %	0.01
Benzene	mol %	0.03
Toluene	mol %	0.02
m-Xylene	mol %	0.01

$$En_{\text{specific}} = \frac{\dot{W}_{\text{comp}}^{\text{total}} + \dot{Q}_{\text{Col}-1}}{\dot{m}_{\text{NGL}} + \dot{m}_{\text{LNG}}} \tag{1}$$

Although heat is included in the specific energy consumption, the thermodynamic value of heat varies depending on the temperature. Thus, the direct summation of heat and work will result in an inaccurate thermodynamic evaluation of the system. In addition, the two products (NGL and LNG) will have changes in temperature, pressure, and composition during optimization. This variation will not be reflected in the energy performance indicator.

Thus, exergy will be an alternative to the energy performance indicator to consider all quality changes in the heat and the products. Exergy is the maximum available work obtained by bringing a system to equilibrium with its environment based on temperature, pressure, and composition [29]. Thus, all quality variations in process streams and different energy forms can be measured by exergy, resulting in a reliable indicator of thermodynamic performance.

Exergy analysis has mostly been used as a post-design tool for NGL extraction systems to find the sources of irreversibilities and measure the improvement of the processes [5,9,15,26,30]. In contrast, there has been one study using the total exergy loss in NGL recovery processes as objective function to optimize such complex systems [9]. However, similar to the energy performance indicator, exergy loss does not consider the quality of the products, thus still giving inaccurate optimization solutions.

Therefore, in this work, an exergy efficiency (extended Exergy Transfer Effectiveness - *ETE*) is used as a performance indicator to optimize the NGL-LNG production systems [17]. This consumed-produced type of exergy efficiency properly reflects the changes in both thermo-mechanical (temperature and pressure) and chemical quality of the products.

For the calculation of the *ETE*, exergy is decomposed into four elements reflecting the work potential of temperature, pressure, composition, and reaction ($\dot{E}^{T}$, $\dot{E}^{P}$, $\dot{E}^{Comp}$, $\dot{E}^{Reac}$) in a stream, which is the exergy classification suggested by Marmolejo-Correa and Gundersen [31].

Disregarding kinetic, potential, electrical and nuclear exergies, the exergy of a stream is composed of two parts, thermo-mechanical exergy ($\dot{E}^{TM}$) and chemical exergy ($\dot{E}^{Ch}$) as seen in Eq. (2) [32].

$$\dot{E}^{\text{Total}} = \dot{E}^{\text{TM}} + \dot{E}^{\text{Ch}} \tag{2}$$

Thermo-mechanical exergy, which is the work produced in reversible processes when bringing the stream to its environment temperature and pressure, is given by:

$$\dot{E}^{\text{TM}} = \dot{H}(T,p) - \dot{H}(T_0,p_0) - T_0[\dot{S}(T,p) - \dot{S}(T_0,p_0)] \tag{3}$$

Thermo-mechanical exergy also has two elements; temperature based exergy ($\dot{E}^{T}$) and pressure based exergy ($\dot{E}^{P}$) as seen in Eq. (4), and they can be defined by Eq. (5) and Eq. (6).

$$\dot{E}^{\text{TM}} = \dot{E}^{\text{T}} + \dot{E}^{\text{P}} \tag{4}$$

$$\dot{E}^{\text{T}} = \dot{H}(T,p) - \dot{H}(T_0,p) - T_0[\dot{S}(T,p) - \dot{S}(T_0,p)] \tag{5}$$

$$\dot{E}^{\text{P}} = \dot{H}(T_0,p) - \dot{H}(T_0,p_0) - T_0[\dot{S}(T_0,p) - \dot{S}(T_0,p_0)] \tag{6}$$

Chemical exergy represents the available work produced in reversible processes when bringing the stream to equilibrium with the chemical composition of the environment under ambient

temperature and pressure. Chemical exergy is composed of two parts, compositional exergy ($\dot{E}^{\mathrm{Comp}}$) and reactional exergy ($\dot{E}^{\mathrm{Reac}}$).

$$\dot{E}^{\mathrm{Ch}} = \dot{E}^{\mathrm{Comp}} + \dot{E}^{\mathrm{Reac}} \tag{7}$$

Compositional exergy, also referred to as mixing exergy, is the reversible work consumed to separate a mixture stream into pure chemical components (i) as defined in Eq. (8) [33,34].

$$\begin{aligned}\dot{E}^{\mathrm{Comp}} &= \dot{H}(T_0,p_0) - \sum_i x_i \dot{H}_i^{\mathrm{pure}}(T_0,p_0) - T_0\left[\dot{S}(T_0,p_0)\right. \\ &\quad \left. - \sum_i x_i \dot{S}_i^{\mathrm{pure}}(T_0,p_0)\right] \\ &= \mathrm{R}T_0 \sum_i \dot{n}_i \ln x_i \ \text{ for ideal gas and ideal mixture}\end{aligned} \tag{8}$$

Reactional exergy is the available work obtained by the reaction of chemical components shifting them into the components that exist in the environment. Reactional exergy of a chemical component at ambient conditions is often referred to as standard chemical exergy ($\overline{e}_{i,0}^{\mathrm{Chem}}$) [35].

$$\dot{E}^{\mathrm{Reac}} = \Sigma x_i \dot{n}_i \overline{e}_{i,0}^{\mathrm{Chem}} \tag{9}$$

Heat can also be regarded as a source of work, and the exergy of heat is defined by the Carnot factor as seen in Eq. (10).

$$\dot{E}^{\mathrm{Q}} = \dot{Q} \times \left(1 - \frac{T_0}{T}\right) \tag{10}$$

In this study, however, the exergy of heat ($\dot{E}^{\mathrm{Q}}$) supplied to the reboiler is calculated by the exergy difference of the steam that passes a heat exchanger having the heat duty Q. The *ETE* is defined by the ratio between exergy sinks and exergy sources as indicated by Eq. (11).

$$ETE = \frac{\sum \text{Exergy Sinks}}{\sum \text{Exergy Sources}} \tag{11}$$

An exergy increase through a process is considered an exergy sink, while a decrease in exergy represents an exergy source. Thus, compression work will be an exergy source, while expansion work is an exergy sink. In addition, the heat consumed in the reboiler will be an exergy source.

$$ETE = \frac{\sum_j \left(\Delta \dot{E}^j\right)^+ + \dot{W}_{\mathrm{exp}}}{\sum_j \left(\Delta \dot{E}^j\right)^- + \dot{E}^{\mathrm{Q}}_{\mathrm{reb}} + \dot{W}_{\mathrm{comp}}} \tag{12}$$

where

$$\left(\Delta \dot{E}^j\right)^+ = \begin{cases} \sum_m \dot{E}^j_m - \sum_k \dot{E}^j_k & \text{if } \sum_k \dot{E}^j_k < \sum_m \dot{E}^j_m \\ 0 & \text{if } \sum_k \dot{E}^j_k > \sum_m \dot{E}^j_m \end{cases} \tag{13}$$

$$\left(\Delta \dot{E}^j\right)^- = \begin{cases} 0 & \text{if } \sum_k \dot{E}^j_k < \sum_m \dot{E}^j_m \\ \sum_k \dot{E}^j_k - \sum_m \dot{E}^j_m & \text{if } \sum_k \dot{E}^j_k > \sum_m \dot{E}^j_m \end{cases} \tag{14}$$

The extended *ETE* with the four exergy components ($\dot{E}^{\mathrm{T}}$, $\dot{E}^{\mathrm{P}}$, $\dot{E}^{\mathrm{Comp}}$, $\dot{E}^{\mathrm{Reac}}$) and the exergy of heat are defined by Eqs. 12–14, where $j \in C, k \in I,\ m \in O$. C is the set of four exergy components, I is the set of inlet streams, and O is the set of outlet streams.

Thus, with the two suggested performance parameters (En_{specific} and *ETE*), optimization studies were conducted with the problem formulation provided by Eqs. (15)-(17).

$$\begin{aligned}&\min_{\mathbf{x}} f(\mathbf{x}) = \mathrm{Obj}_1(\mathbf{x}) \vee \mathrm{Obj}_2(\mathbf{x}) \\ &\text{subject to } \Delta T_{\mathrm{min,a}}(\mathbf{x}) \geq 3 \ a = \{\mathrm{HE}-1,2,3,4\} \\ &\quad \Delta T_{\mathrm{sup,b}}(\mathbf{x}) \geq 0 \ b = \{\mathrm{W04},\ \mathrm{C06}\} \\ &\quad 1 \leq Pr_c(\mathbf{x}) \leq 4 \ c = \{\mathrm{K}-1,2,3,4,5,6\} \\ &\quad x^{\mathrm{LNG}}_{\mathrm{N_2}}(\mathbf{x}) \leq 1 \text{ mol\%} \\ &\quad \sum_d x^{\mathrm{Col}-1\,\mathrm{vap}}_d(\mathbf{x}) \leq 0.1 \text{ mol \% } d = \{\mathrm{i}-\mathrm{C_5}, \mathrm{n}-\mathrm{C_5} \ldots, \mathrm{m}-\mathrm{Xylene}\} \\ &\quad \sum_e x^{\mathrm{Col}-1\,\mathrm{vap}}_e(\mathbf{x}) \leq 10 \text{ ppm } \ e = \{\mathrm{Benzene}, \mathrm{Toluene}, \mathrm{m}-\mathrm{Xylene}\} \\ &\quad \mathbf{x}_{\mathrm{LB}} \leq \mathbf{x} \leq \mathbf{x}_{\mathrm{UB}}\end{aligned} \tag{15}$$

where

$$\mathrm{Obj}_1 = En_{\mathrm{specific}}(\mathbf{x}) \tag{16}$$

$$\mathrm{Obj}_2 = ETE(\mathbf{x}) \tag{17}$$

Optimization was performed using a local solver based on a sequential quadratic programming (SQP) algorithm in Matlab. The SQP algorithm uses the Lagrangian function handling both the objective function and constraints with Lagrangian multipliers. Stopping criteria for the SQP is listed in Table 3. The simulation models in HYSYS are connected to Matlab through the ActiveX Component Object Model server for the communication between the process simulator and the optimization algorithm. Objective and constraint values such as exergy efficiency, specific energy consumptions and degree of superheating are obtained from HYSYS by using its internal calculation sheets and Visual Basic for Applications programming and sent to Matlab for optimization, requiring a total optimization run time of over 30 min.

During the optimization, all product specifications mentioned in Section 4.2 are regarded as constraints. In order to address the trade-off between thermodynamic performance and cost of heat exchangers, the minimum temperature difference is set to be 3 K [36,37]. The degree of superheating for the compressor inlet streams is also constrained to be larger than zero Kelvin to protect compressor blades from droplets. The maximum pressure ratio of compressors is limited to be less than 4 due to practical issues [38].

The decision variables and the optimization results for the NGL and LNG production systems are shown in Table 4 with corresponding constraint values in Table 5. The composition of the two refrigerants and their pressure levels in the DMR process are selected as decision variables for the natural gas liquefaction part. In addition, pre-cooling, liquefaction and sub-cooling temperature (heat exchanger outlet temperatures) of natural gas are varied since they affect the performance of the LNG process and also the HHC separation.

For the distillation column, the methane mole fraction of the bottom product is selected as an optimization variable so that the degree of separation through the column can be easily controlled. Besides, the upper bound of the methane mole fraction will limit methane slip to the NGL product without additional constraints. The pressure level of the column is also varied to be below critical pressure in order to have a proper separation performance. The outlet pressure level of the boost compressor for the distillation top

Table 3
Parameters for SQP used in this work.

Maximum iteration	Maximum function evaluation	Function tolerance	Constraint violation tolerance
1000	2000	10^{-8}	10^{-4}

Table 4
Bounds for the decision variables and the best solutions for the integrated schemes.

Variable	Unit	Bound		ISS-LNG		NGL-LNG		Refluxed NGL-LNG	
		LB	UB	Obj_1	Obj_2	Obj_1	Obj_2	Obj_1	Obj_2
$\dot{n}_{C_1,WMR}$	kmol/hr	1000	13,000	5969	3778	7165	4638	3126	2487
$\dot{n}_{C_2,WMR}$	kmol/hr	20,000	38,000	29,982	25,590	32,335	28,168	29,775	25,935
$\dot{n}_{C_3,WMR}$	kmol/hr	2000	14,000	9547	12,555	13,597	10,792	8103	9472
$\dot{n}_{nC_4,WMR}$	kmol/hr	100	9000	5621	6558	6508	7545	8472	8131
$\dot{n}_{N_2,CMR}$	kmol/hr	1000	10,000	1997	2001	1992	1997	1986	2021
$\dot{n}_{C_1,CMR}$	kmol/hr	10,000	25,000	17,737	18,449	19,118	18,628	19,094	19,043
$\dot{n}_{C_2,CMR}$	kmol/hr	10,000	25,000	19,724	18,831	18,897	19,588	20,956	20,659
$\dot{n}_{C_3,CMR}$	kmol/hr	500	12,000	4896	6434	4818	5232	3246	3747
$p_{LP,WMR}$	bar	5.00	15.00	12.07	9.65	11.42	9.61	7.25	6.36
$p_{MP,WMR}$	bar	15.00	25.00	22.88	17.28	20.26	18.33	17.47	17.54
$p_{HP,WMR}$	bar	25.00	55.00	36.87	27.18	30.30	29.96	30.35	30.10
$p_{LLP,CMR}$	bar	2.00	8.00	4.40	4.05	4.96	4.31	4.95	4.58
$p_{LP,CMR}$	bar	8.00	20.00	17.37	16.34	14.77	15.89	19.66	18.31
$p_{MP,CMR}$	bar	20.00	35.00	27.22	27.85	24.02	25.88	27.78	27.92
$p_{HP,CMR}$	bar	35.00	60.00	40.94	41.01	41.22	39.80	38.12	37.53
$T_{HE-1,\ out}$	°C	−55.00	−30.00	−34.18	−31.54	−35.55	−35.07	−41.01	−41.05
$T_{HE-2,\ out}$	°C	−135.00	−110.00	−117.38	−118.85	−113.64	−117.52	−115.42	−116.89
$T_{HE-3,\ out}$	°C	−160.00	−145.00	−145.00	−149.23	−145.00	−148.28	−145.00	−147.50
$T_{HE-4,\ out}$	°C	−40.00	−10.00	−30.85	−30.84	–	–	−19.25	−19.92
$x_{C_1,NGL}$	mol %	0.00	5.00	5.00	0.83	5.00	2.71	5.00	2.99
p_{Col-1}	bar	30.00	55.00	43.75	43.88	43.59	43.09	55.00	55.00
p_{K-6}	bar	50.00	70.00	58.29	60.37	63.55	58.66	55.48	55.00
Tee − 1[a]	–	0.75	1.00	–	–	–	–	0.86	0.86

[a] Flow ratio from W01 to W02a.

Table 5
Constraint values from the best solutions of the integrated schemes with different objective functions.

Parameter	Unit	ISS-LNG		NGL-LNG		Refluxed NGL-LNG	
		Obj_1	Obj_2	Obj_1	Obj_2	Obj_1	Obj_2
$\Delta T_{min,HE-1}$	°C	3.00	3.00	3.00	3.00	3.00	3.00
$\Delta T_{min,HE-2}$	°C	3.00	3.00	3.00	3.00	3.00	3.00
$\Delta T_{min,HE-3}$	°C	3.00	3.00	3.00	3.00	3.00	3.00
$\Delta T_{min,HE-4}$	°C	3.00	3.00	–	–	3.00	3.00
$\Delta T_{sup,W04}$	°C	0.16	0.23	0.52	0.27	0.11	0.06
$\Delta T_{sup,C06}$	°C	13.13	14.34	27.05	23.65	9.36	9.44
Pr_{K-1}	–	1.90	1.79	1.77	1.91	2.41	2.76
Pr_{K-2}	–	1.61	1.57	1.50	1.63	1.74	1.72
Pr_{K-3}	–	3.95	4.03	2.98	3.69	3.97	4.00
Pr_{K-4}	–	1.57	1.70	1.63	1.63	1.41	1.52
Pr_{K-5}	–	1.50	1.47	1.72	1.54	1.37	1.34
Pr_{K-6}	–	1.18	1.22	1.46	1.36	1.01	1.00
$x_{C_{5+}}$	mol %	0.04	0.04	0.04	0.04	0.08	0.07
x_{BTX}	ppm	9.8	10	10	10	10	9.8

vapor product is selected as a decision variable since feed gas pressure level has a considerable effect on the thermodynamic efficiency of the liquefaction. In this work, the number of trays and the location of feed streams to the distillation column are not selected as decision variables since the optimal column design is not the scope of this study. Detailed operating conditions are listed in Table S1 to Table S6 in Appendix A.

6. Results

In this work, the DMR process with upstream or integrated NGL extraction was optimized and compared based on two performance indicators (specific energy consumption and exergy efficiency). All processes also fulfilled the constraints such as C_{5+} and BTX contents in the vapor stream entering the liquefaction system.

The optimization results with the energy performance indicator (Obj_1 in Table 6) shows that the refluxed NGL-LNG process has the smallest specific energy consumption. The upstream NGL extraction system (ISS-LNG process) also indicates a low specific energy consumption, having a marginal difference compared to the refluxed NGL-LNG system. The simple integrated scheme of NGL and LNG production (NGL-LNG system), however, has the largest specific energy consumption. This large energy consumption indicates that the integration may not be thermodynamically

Table 6
Performance parameters with different objective functions for the integrated schemes.

Parameter	Unit	ISS-LNG		NGL-LNG		refluxed NGL-LNG	
		Obj_1	Obj_2	Obj_1	Obj_2	Obj_1	Obj_2
$En_{specific}$	kWh/ton	214.98	216.55	221.49	222.32	214.88	216.65
ETE	%	68.97	69.50	67.70	68.12	69.05	69.23
$\dot{W}_{comp}^{total}$	MW	118.73	122.21	122.39	125.36	119.24	121.77
$\dot{Q}_{Reb-1}$	MW	5.03	5.80	4.97	5.32	4.47	5.01
$\dot{E}^{\dot{Q}_{Reb-1}}$	MW	1.16	1.60	1.15	1.36	1.54	1.84

Table 7
Products of the NGL and LNG systems with specific energy consumption per unit calorific value of the products.

Parameter	Unit	ISS-LNG		NGL-LNG		Refluxed NGL-LNG	
		Obj_1	Obj_2	Obj_1	Obj_2	Obj_1	Obj_2
NGL	kmol/s	0.23	0.22	0.23	0.22	0.14	0.13
LHV_{NGL}	MJ/kmol	2431.61	2507.93	2438.12	2485.12	2781.35	2816.62
LHV_{NGL}	MW	566.63	555.79	562.06	553.91	377.37	377.43
LNG	kmol/s	8.54	8.82	8.54	8.76	8.64	8.81
LHV_{LNG}	MJ/kmol	852.63	850.56	853.00	851.38	864.94	863.19
LHV_{LNG}	MW	7285.42	7499.85	7281.23	7458.53	7475.82	7600.40
End-flash gas	kmol/s	0.94	0.68	0.96	0.74	0.94	0.78
$LHV_{End-flash\ gas}$	MJ/kmol	743.92	730.63	744.38	733.92	743.63	736.01
$LHV_{End-flash\ gas}$	MW	702.64	499.04	711.39	542.25	701.49	576.29
$\frac{\dot{W}_{comp} + \dot{Q}_{Reb-1}}{LHV_{total}}$ [a]	–	0.0145	0.0150	0.0149	0.0153	0.0145	0.0148

[a] $LHV_{total} = LHV_{NGL} + LHV_{LNG} + LHV_{End-flash\ gas}$.

advantageous compared to the upstream HHC extraction when the NGL recovery system is not thoroughly heat integrated with the liquefaction system.

In the case of the refluxed NGL-LNG system, the condenser part of the NGL extraction column (Col-1) is integrated with the DMR process, allowing the column to have a reflux stream from the top vapor product. This reflux increases the separation performance of the distillation column, which enables the process unit to operate at a higher pressure than the equipment in the NGL-LNG system as seen in Table 4. Therefore, the refluxed NGL-LNG system requires less compression power to compensate for the reduced pressure level of the feed gas compared to the simple integrated scheme. Thus, the boost compressor (K-6) in the refluxed process is not needed, since its pressure ratio has a value very close to one (Pr_{K-6} in Table 5).

The operating pressure level of the column in the NGL-LNG system is even lower than the ISS-LNG process, which will require a larger duty of the boost compressor and thus the largest specific energy consumption compared to the other systems. In the same way as for the energy performance indicator, the ISS-LNG and the refluxed NGL-LNG systems achieved the highest exergy efficiency values of 69.50% and 69.23% respectively, while the NGL-LNG process obtained an *ETE* value of 68.12%.

The results also clearly show that minimizing specific energy consumption (Obj_1) gives different values of the two performance indicators compared to the ones obtained by maximizing exergy efficiency (Obj_2). Minimizing specific energy consumption results in a penalty in exergy efficiency between 0.18 and 0.52% points for the three process configurations, while maximizing exergy efficiency results in a penalty in specific energy consumption between 0.83 and 1.77 kWh/ton. However, the differences in specific energy consumption and exergy efficiency values between the optimization results from the two objective functions (Obj_1 and Obj_2) are marginal. The largest increase in specific energy consumption when using exergy efficiency as the objective function is 0.82% for the refluxed NGL-LNG, while the largest decrease in exergy efficiency when using specific energy consumption as the objective function is 0.76% for the ISS-LNG process.

From the results of energy and exergy based optimization, it can be concluded that the changes in operating conditions for the systems are significant and meaningful. Especially, Table 6 indicates the noticeable increase in column reboiler duty and compression power for the three process configurations when switching objective function from energy to exergy. This behavior can be explained by the best solutions of the decision variables from the minimization results with Obj_2. First, Table 4 indicates that the minimization of the *ETE* results in a lower methane fraction in the NGL product for all the systems compared to the results from Obj_1. Thus, the NGL product becomes richer in heavier hydrocarbons, while having leaner LNG product as seen in the low heating values (LHV) in Table 7. This means that the *ETE* objective function guides the process towards a higher HHC separation efficiency.

Although the sharper separation gives a larger reboiler duty and a smaller production of NGL due to the evaporation of methane, this is compensated by the higher heating value of the NGL and the larger production of LNG. Thus, as seen in Table 7, there is a minor difference in the lower heating value (LHV) of the NGL between the results from the two objective functions. Besides, the actual value of the additional heat input to the reboiler (exergy of heat) is half of the increment in heat duty, which will be an acceptable increase for the deeper separation.

In contrast, Table 4 indicates that the objective function based on the energy performance parameter resulted in the methane fraction in the NGL product reaching its upper bound. Since the specific energy consumption is unable to measure the compositional quality change and thus the separation performance, the objective function leads the NGL and LNG production systems to have the reboiler duty as small as possible by allowing a larger methane fraction in the NGL. Although the optimization using the energy performance indicator succeeded in reducing the total energy consumption, Obj_1 allows the systems to have a larger amount of methane slip through the NGL product.

Table 4 also shows that all the systems optimized according to exergy efficiency have a lower outlet temperature from the last heat exchanger in the DMR system ($T_{HE-3,\ out}$) compared to the results from minimization of specific energy consumption. This temperature reduction increases the cold duty of the liquefaction process and thus the power consumption, as seen in Table 6.

However, the colder outlet temperature of HE-3 gives a larger degree of sub-cooling in the liquefied natural gas stream. This colder LNG stream results in a larger fraction of liquid product after being throttled to around ambient pressure. Thus, as seen in Table 7, the *ETE* objective function increases the final LNG product by decreasing the outlet temperature of HE-3, while reducing the end-flash vapor, compared to the results from minimization with Obj_1.

The main reason for the larger production of the final LNG is that the exergy efficiency measures the quality of the products (NGL, LNG, and end-flash vapor). This is in contrast to the specific energy consumption that only considers total energy consumption and mass flow rates of NGL and LNG. As seen in Table 8, the molar temperature based exergy value of the final LNG product is significantly larger than the end-flash vapor since the liquid product has latent heat to be utilized as cold energy.

Therefore, the optimization based on the *ETE* objective function

Table 8
Molar temperature based exergy of the final LNG product from the optimization results using different objective functions.

Parameter	Unit	ISS-LNG		NGL-LNG		refluxed NGL-LNG	
		Obj_1	Obj_2	Obj_1	Obj_2	Obj_1	Obj_2
$T_{\text{cold products}}$ [a]	°C	−156.7	−157.0	−156.7	−156.9	−156.6	−156.8
$\dot{e}^{T}_{LNG}$	kJ/kmol	15865.0	15890.9	15863.4	15883.7	15835.9	15852.2
$\dot{e}^{T}_{\text{End-flash vapor}}$	kJ/kmol	3310.4	3315.8	3310.0	3314.2	3303.9	3307.3

[a] LNG and end-flash vapor.

leads the system to have a lower sub-cooling temperature for larger production of LNG, which increases the total exergy value of the two products. The reduction in the outlet temperature of HE-3 also increases the molar temperature based exergy of the final LNG and end-flash vapor, thus increasing the produced exergy.

In contrast, the optimization using Obj_1 forced the sub-cooling temperature to be as warm as possible, reaching the upper bound as seen in Table 4. As a result, the refrigeration duty and the compression work were decreased, while the production of the final LNG was reduced. Since the effect of decreasing work consumption was larger than the effect of product reduction in the specific energy consumption, the system was optimized to have a warm outlet temperature from the liquefaction process. Thus, the energy based objective function did not maximize the LNG product since the specific energy consumption ignores the thermodynamic quality of this liquid stream. Instead, the optimization with Obj_1 allowed the system to have a larger amount of end-flash gas although the gas stream was disregarded as a product in the formulation of the specific energy consumption. The higher economic value of the final LNG compared to the end-flash vapor also indicates that a smaller production of the liquid product is not a favorable solution for this system.

To include the quality of the NGL and LNG in the energy performance indicator, the calorific value of the two products can substitute the mass flow rates in the formulation of the specific energy consumption [39] as seen in Table 7. This performance indicator shows that the operating conditions from Obj_2 give a larger energy consumption per calorific value than the one from Obj_1. This result does not mean the operating conditions from Obj_1 is thermodynamically better since the performance indicator with the heating values only reflects the changes in chemical energy of the products, while the temperature, pressure, and compositional changes are not covered.

7. Discussion

In this work, two different objective functions, specific energy consumption and exergy efficiency, have been applied in the optimization of systems for LNG and NGL production in order to evaluate the effectiveness of the two different performance indicators for complex systems.

The optimization results using the specific energy consumption as objective function indicate that the LNG process integrated with the NGL extraction using a refluxed column has the lowest specific energy consumption and a high exergy efficiency. However, the operating conditions from the minimization studies using the energy performance indicator show that the systems were optimized to maximize the methane content in the NGL product. Although the reboiler duty of the distillation column was decreased due to the high methane fraction allowed in the NGL, the methane product (LNG) was also reduced, meaning a lower HHC separation performance of the system. Besides, the degree of sub-cooling in the natural gas stream is minimized to decrease the refrigeration duty and its compressor work. The low degree of sub-cooling results in a smaller production of the liquid stream (LNG) after the sub-cooled natural gas stream is throttled to ambient pressure. Although the specific energy consumption focuses on the production of NGL and LNG, this performance indicator guided the system to produce a larger amount of end-flash gas, which is less valuable than the LNG product.

Unlike the energy performance indicator, the minimization of the *ETE* results in a smaller methane fraction in the NGL product by having a larger reboiler duty. However, the additional reboiler duty is compensated by the increased heating value of the NGL product and the increase in LNG production since more methane ends up there. Therefore, the exergy efficiency is able to manipulate the operating conditions to have a higher HHC separation performance.

Besides, the objective function based on the *ETE* succeeds in maximizing the LNG by lowering the sub-cooling temperature of the natural gas, while reducing the end-flash vapor. A higher thermodynamic (exergy) value of the LNG product compared to the end-flash vapor is the main reason for the exergy based objective function to guide the system towards having a larger degree of sub-cooling. Thus, the optimization using exergy efficiency results in more favorable operating conditions for the NGL and LNG production systems since it reflects the HHC separation performance and the thermodynamic value of the LNG cold energy.

Based on the discussion above, exergy efficiency will be the most suitable objective function to optimize the complex distillation and liquefaction system since this indicator can reflect both the separation performance and the thermodynamic quality of the products. Thus, this performance indicator results in processes where the amount of NGL production is maintained with a lower methane content, and the amount of the LNG product is maximized while reducing the end-flash vapor, which has lower thermodynamic and economic values.

8. Conclusions

The DMR process with upstream or integrated NGL extraction has been optimized in order to evaluate and compare different NGL extraction schemes. During optimization of the NGL and LNG production systems, a generalized exergy efficiency (extended *ETE*) has been used as the main objective function. This key performance indicator is shown to be superior to energy based performance indicators, since exergy correctly measures the thermodynamic quality of energy forms and material products.

Based on the optimization results using the extended *ETE*, none of the two configurations having the NGL extraction integrated with the DMR process perform thermodynamically better than the liquefaction system with upstream HHC recovery. Thus, these integrated schemes of the NGL and LNG processes will not be favorable unless further development is made for the integrated system. Although the difference in the exergy efficiency between the schemes with upstream and integrated HHC recovery is only marginal, more advanced upstream NGL extraction technologies such as the gas sub-cooled and the recycle split vapor processes will increase the performance difference, making the integrated

systems even less attractive.

Declaration of competing interests

The authors declare that they have no known competing financial interests or personal relationships that could have appeared to influence the work reported in this paper.

Acknowledgements

The authors would like to acknowledge Statoil (now Equinor) for financial support.

Appendix A. Supplementary data

Supplementary data to this article can be found online at https://doi.org/10.1016/j.energy.2020.117232.

Nomenclature

Abbreviations

BTX	benzene, toluene, and xylene
CMR	cold mixed refrigerant
DMR	dual mixed refrigerant
EOS	equation of state
GSP	gas sub-cooled process
HHC	heavier hydrocarbon
ISS	industry standard single stage process
JT	Joule-Thomson
KPI	key performance indicator
LB	lower bound
LHV	lower heating value
LNG	liquefied natural gas
NGL	natural gas liquid
RSV	recycled split vapor process
SQP	sequential quadratic programming
UB	upper bound
WMR	warm mixed refrigerant

Roman symbols

$\dot{E}$	exergy rate [kW]
$\bar{e}$	molar exergy [kJ/kmol]
En	energy consumption [kW]
ETE	exergy transfer effectiveness [%]
$\dot{H}$	enthalpy rate [kW]
$\dot{m}$	mass flow rate [kg/s]
$\dot{n}$	molar flow rate [kmol/s]
p	pressure [bar]
Pr	pressure ratio [−]
$\dot{Q}$	heat rate [kW]
$\dot{S}$	entropy rate [kW/K]
T	temperature [K]
$\dot{W}$	work [kW]
$\mathbf{x}$	decision variables
x	fraction [−]

Greek symbols

$\Delta T_{\min}$	heat exchanger minimum approach temperature [°C]
$\Delta T_{\sup}$	degree of superheating [°C]

Subscripts and superscripts

0	ambient conditions
BTX	sum of benzene, toluene, and xylene mole fraction
C5+	sum of hydrocarbon mole fractions heavier than pentane
Ch	chemical exergy
Chem	standard chemical exergy
Comp	compositional exergy
comp	compressor
exp	expander
LB	lower bound
LNG	liquefied natural gas
NGL	natural gas liquids
P	pressure based exergy
pure	pure component stream
Q	exergy of heat
Reac	reactional exergy
reb	reboiler
specific	specific consumption
T	temperature based exergy
TM	thermo-mechanical exergy
total	total compression power
Total	total exergy of a stream
UB	upper bound
vap	vapor

References

[1] IGU. 2019 World LNG Report. In: World gas conference. Fornebu, Norway: International Gas Union (IGU); 2019.
[2] Bucklin RW. Method and equipment for treating hydrocarbon gases for pressure reduction and condensate recovery. U.S. Patent No. 3,292,380; 1966.
[3] Campbell RE, Wilkinson JD. Hydrocarbon gas processing. U.S. Patent No. 4,278,457; 1981.
[4] Campbell RE, Wilkinson JD, Hudson HM. Hydrocarbon gas processing. U.S. Patent No. 5,568,737; 1994.
[5] Ghorbani B, Shirmohammadi R, Mehrpooya M. A novel energy efficient LNG/NGL recovery process using absorption and mixed refrigerant refrigeration cycles – economic and exergy analyses. Appl Therm Eng 2018;132:283–95.
[6] Ghorbani B, Hamedi M-H, Amidpour M. Development and optimization of an integrated process configuration for natural gas liquefaction (LNG) and natural gas liquids (NGL) recovery with a nitrogen rejection unit (NRU). J Nat Gas Sci Eng 2016;34:590–603.
[7] Uwitonze H, Lee I, Hwang KS. Alternatives of integrated processes for coproduction of LNG and NGLs recovery. Chem Eng Process: Process Intensification 2016;107:157–67.
[8] Khan MS, Chaniago YD, Getu M, Lee M. Energy saving opportunities in integrated NGL/LNG schemes exploiting: thermal-coupling common-utilities and process knowledge. Chem Eng Process: Process Intensification 2014;82:54–64.
[9] Shin J, Yoon S, Kim J-K. Application of exergy analysis for improving energy efficiency of natural gas liquids recovery processes. Appl Therm Eng 2015;75:967–77.
[10] Park JH, Khan MS, Andika R, Getu M, Bahadori A, Lee M. Techno-economic evaluation of a novel NGL recovery scheme with nine patented schemes for offshore applications. J Nat Gas Sci Eng 2015;27:2–17.
[11] Kim S, Nam K, Byun WY. Selection study on natural gas liquid extraction processes in offshore plants. In: Proceedings of the 24th international ocean and polar engineering conference (ISOPE 2014). Busan, korea. International Society of Offshore and Polar Engineers (ISOPE); 2014.
[12] Jin C, Lim Y. Economic evaluation of NGL recovery process schemes for lean feed compositions. Chem Eng Res Des 2018;129:297–305.
[13] Mehrpooya M, Vatani A, Ali Mousavian SM. Introducing a novel integrated NGL recovery process configuration (with a self-refrigeration system (open–closed cycle)) with minimum energy requirement. Chem Eng Process: Process Intensification 2010;49(4):376–88.
[14] Vatani A, Mehrpooya M, Tirandazi B. A novel process configuration for co-production of NGL and LNG with low energy requirement. Chem Eng Process: Process Intensification 2013;63:16–24. 0.
[15] He T, Ju Y. Design and optimization of a novel mixed refrigerant cycle integrated with NGL recovery process for small-scale LNG plant. Ind Eng Chem Res 2014;53(13):5545–53.
[16] Yoon S, Binns M, Park S, Kim J-K. Development of energy-efficient processes for natural gas liquids recovery. Energy 2017;128:768–75.
[17] Kim D, Gundersen T. Development and use of exergy efficiency for complex cryogenic processes. Energy Convers Manag 2018;171:890–902.
[18] Kim D, Giametta REH, Gundersen T. Optimal use of liquefied natural gas (LNG) cold energy in air separation units. Ind Eng Chem Res 2018;57(17):5914–23.
[19] Mak J. Configurations and methods for offshore NGL recovery. U.S. Patent No. 20140060114 A1; 2014.

[20] Roberts MJ, Agrawal R. Dual mixed refrigerant cycle for gas liquefaction. U.S. Patent No. 6,269,655 B1; 2001.
[21] Grootjans HF, Nagelvoort RK, Vink KJ. Liquefying a stream enriched in methane. U.S. Patent No. 6,370,910 B1; 2002.
[22] Aspen Technology Inc. Aspen HYSYS V9. 2016.
[23] Chen F, Ott CM. Lean gas. LNG Industry; 2013. JanFeb.
[24] Ghorbani B, Hamedi M-H, Amidpour M, Shirmohammadi R. Implementing absorption refrigeration cycle in lieu of DMR and C3MR cycles in the integrated NGL, LNG and NRU unit. Int J Refrig 2017;77:20–38.
[25] Ghorbani B, Hamedi M-H, Amidpour M, Mehrpooya M. Cascade refrigeration systems in integrated cryogenic natural gas process (natural gas liquids (NGL), liquefied natural gas (LNG) and nitrogen rejection unit (NRU)). Energy 2016;115:88–106.
[26] Mehrpooya M, Hossieni M, Vatani A. Novel LNG-based integrated process configuration alternatives for coproduction of LNG and NGL. Ind Eng Chem Res 2014;53(45):17705–21.
[27] Lee S, Long NVD, Lee M. Design and optimization of natural gas liquefaction and recovery processes for offshore floating liquefied natural gas plants. Ind Eng Chem Res 2012;51(30):10021–30.
[28] Lior N, Zhang N. Energy, exergy, and Second Law performance criteria. Energy 2007;32(4):281–96.
[29] Szargut J. International progress in second law analysis. Energy 1980;5(8):709–18.
[30] Ghorbani B, Salehi GR, Ghaemmaleki H, Amidpour M, Hamedi MH. Simulation and optimization of refrigeration cycle in NGL recovery plants with exergy-pinch analysis. J Nat Gas Sci Eng 2012;7:35–43.
[31] Marmolejo-Correa D, Gundersen T. A comparison of exergy efficiency definitions with focus on low temperature processes. Energy 2012;44(1):477–89.
[32] Brodyansky VM, Sorin MV, Goff PL. The efficiency of industrial processes: exergy analysis and optimization. Amsterdam: Elsevier; 1994.
[33] Ghannadzadeh A, Thery-Hetreux R, Baudouin O, Baudet P, Floquet P, Joulia X. General methodology for exergy balance in ProSimPlus® process simulator. Energy 2012;44(1):38–59.
[34] Sato N. Chemical energy and exergy. Amsterdam: Elsevier Science B.V.; 2004.
[35] Szargut J. Chemical exergies of the elements. Appl Energy 1989;32(4):269–86.
[36] Austbø B, Gundersen T. Using thermodynamic insight in the optimization of LNG processes. Computer Aided Chemical Engineering 2014;33:1273–8.
[37] Xu X, Liu J, Cao L. Optimization and analysis of mixed refrigerant composition for the PRICO natural gas liquefaction process. Cryogenics 2014;59:60–9.
[38] Finlayson BA. Introduction to chemical engineering computing. Hoboken, NJ, USA: John Wiley & Sons, Inc.; 2012.
[39] Svalheim S, King DC. Life of field energy performance. Proceedings of offshore europe 2003. Aberdeen, United Kingdom: Society of Petroleum Engineers (SPE); 2003. p. 6.